Available online at www.sciencedirect.com

ScienceDirect

Ceramics International 40 (2014) 2511–2517

CERAMICS INTERNATIONAL

www.elsevier.com/locate/ceramint

Short communication

Mechanical properties of nanostructured TiN–AlN composites rapidly consolidated by pulsed current activated sintering

Wonbaek Kim[a], Jae-Won Lim[a], Hyun-Su Oh[b], In-Jin Shon[b,*]

[a]Minerals and Materials Processing Division, Korea Institute of Geoscience, Mining and Materials Resources, Daejeon, Republic of Korea
[b]Division of Advanced Materials Engineering and Center for Advanced Bioimaging Research, Engineering College, Chonbuk National University, Jeonju, Republic of Korea

Received 15 June 2013; received in revised form 18 July 2013; accepted 19 July 2013
Available online 26 July 2013

Abstract

Commercial TiN and AlN powders were high-energy ball milled for various durations and consolidated without a binder using the pulsed current activated sintering method (PCAS). The effects of milling on the sintering behavior, crystallite size and mechanical properties of the TiN–AlN composites were evaluated. A dense nanostructured TiN–AlN composite with a relative density of up to 99% could be readily obtained within 3 min. The ball milling effectively refined the crystallite structure of the TiN and AlN powders and facilitated subsequent densification. The sintering-onset temperature was appreciably reduced by milling for 40 h from 1200 °C to 1000 °C. Accordingly, the relative density of the TiN–AlN composite increased as the milling time was increased. This clearly demonstrates that the quick densification of nanostructured TiN–AlN bulk materials to near the theoretical density could be obtained by the combination of PCAS and the preparatory high-energy ball milling process.

Keywords: A. Sintering; C. Hardness; Nanopowder; TiN–AlN; Nanomaterials

1. Introduction

Nitrides are used in many applications because of their hardness, high-temperature properties and wear resistance. Among the various nitrides, titanium nitride is particularly interesting because of its excellent wear properties and corrosion resistance [1]. Titanium nitride can be produced by the self-propagating high temperature synthesis (SHS) process [2,3]. The combustion synthesis of titanium nitride has usually been conducted under nitrogen gas pressures ranging from 0.1 to 10 MPa. The effects of the nitrogen pressure, pressed sample porosity, and diluent addition on the material stoichiometry have been investigated [4–7].

Dense TiN bodies can be sintered using micron-sized powders and conventional sintering at high temperatures (above 2000 °C). By comparison, the use of nano powders allows sintering at lower temperatures (1300–1500 °C) [8]. Nevertheless, nano powders often present a high oxygen affinity which can be an obstacle in the densification stage [9]. The pulsed-current activated sintering (PCAS) method has recently emerged as an effective technique for the consolidation of high temperature materials which are difficult to sinter without additives because of their high melting point and strong covalent bond [10–12]. We previously investigated the sintering behavior of TiN nanopowders using PCAS. The average crystallite size of the sintered TiN was much larger than that of the nanopowders due to grain growth. This may be attributed to the high grain boundary energy of TiN [13].

Nanocrystalline materials have received much attention as advanced engineering materials with improved physical and mechanical properties [14,15]. Since they possess a high strength and hardness as well as excellent ductility and toughness, they have garnered more attention recently [16,17]. In an effort to sinter nanostructured TiN compacts, a second phase such as AlN has been added to inhibit grain growth. AlN has many attractive properties including a high thermal conductivity, a lower thermal expansion, and other good electrical properties [18].

In this study, we investigated the binderless sintering of TiN–AlN composites using the PCAS method. The effects of preparatory milling on the crystalline size, mechanical properties, and densification behavior of micron-size TiN–AlN powders were evaluated.

*Corresponding author. Tel.: +82 63 270 2381; fax: +82 63 270 2386.
E-mail address: ijshon@chonbuk.ac.kr (I.-J. Shon).

0272-8842/$ - see front matter © 2013 Elsevier Ltd and Techna Group S.r.l. All rights reserved.
http://dx.doi.org/10.1016/j.ceramint.2013.07.090

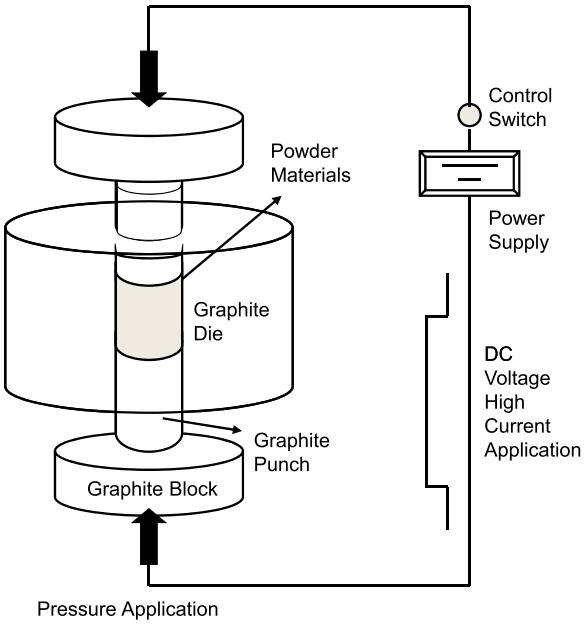

Fig. 1. Schematic of the pulsed-current activated sintering set-up.

2. Experimental procedures

The TiN powders used in this study were supplied by Treibacher Industrie AG (Germany) and had an average particle size of about 1.4 μm with a purity of 99%. The AlN powders were supplied by Aldrich, Inc. and had a grain size of < 10 μm with a purity of 98%. The powders (50 mol%TiN–50 mol% AlN) were first milled in a high-energy ball mill (Pulverisette-5 planetary mill) at 250 rpm for various durations (0, 1, 4, 10, and 40 h). Tungsten carbide balls (9 mm in diameter) were used in a sealed cylindrical stainless steel vial under an argon atmosphere. The balls:powder weight ratio was 30:1. The milling resulted in a significant reduction of the particle size. The crystallite sizes of the TiN and AlN powders were calculated from the full width at half-maximum (FWHM) values of the diffraction peaks by applying Suryanarayana and Grant Norton′s formula [19].

$$B_r(B_{crystalline} + B_{strain})\cos\ \theta = k\lambda/L + \eta \sin\ \theta \quad (1)$$

Here, B_r is the full width at half-maximum (FWHM) of the diffraction peak after instrument correction, $B_{crystalline}$ and B_{strain} are the FWHM values caused by small grain size and internal

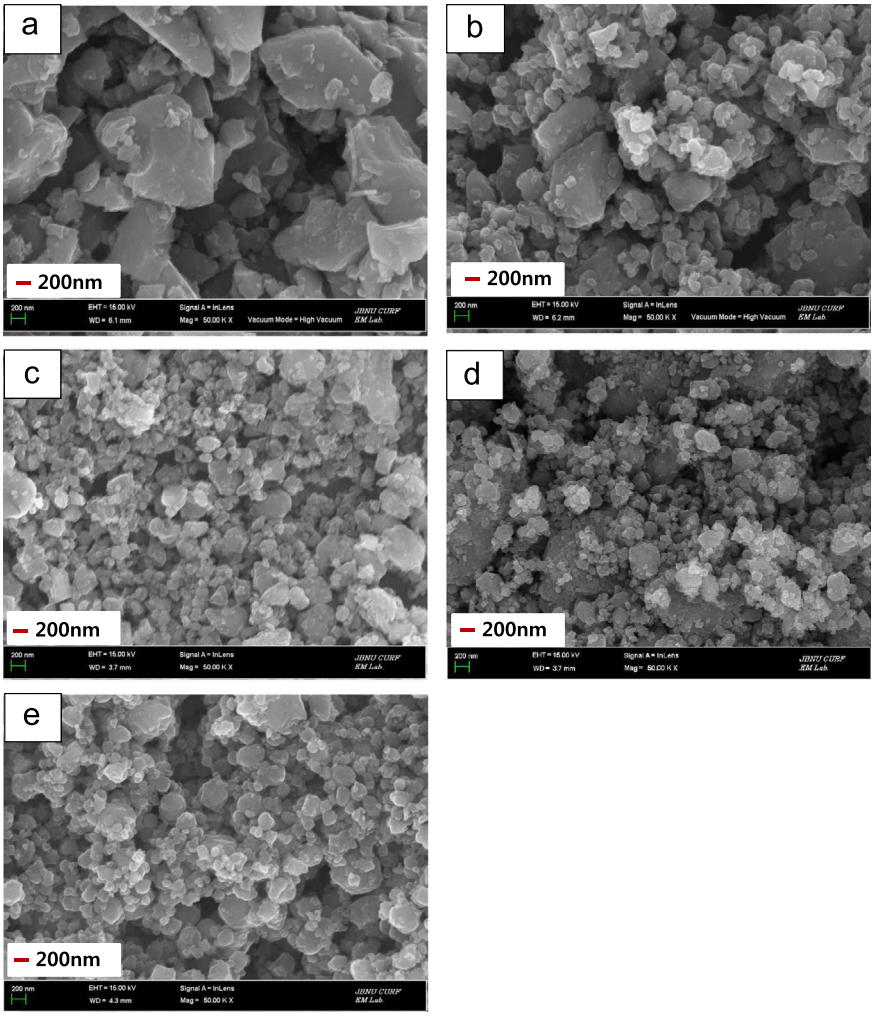

Fig. 2. FE-SEM images of the TiN–AlN powders after high-energy milling for various durations: (a) as-received, (b) milled for 1 h, (c) milled for 4 h, (d) milled for 10 h, and (e) milled for 40 h.

stress, respectively, k is a constant (with a value of 0.9), λ is the wavelength of the X-ray radiation, L and η are the grain size and internal strain, respectively; and θ is the Bragg angle. The parameters B and B_r follow Cauchy′s form with the relationship $B=B_r+B_s$, where B and B_s are the FWHMs of the broadened Bragg peaks and the Bragg peaks of the standard sample, respectively.

The powders were placed in a graphite die (outside diameter of 35 mm, inside diameter of 10 mm, height of 40 mm) and then introduced into the pulsed current activated sintering (PCAS) apparatus, as shown schematically in Fig. 1. The PCAS apparatus includes a 30 kW power supply which provides the pulsed current (on time of 20 μsec, off time of 10 μsec) through the sample and a 50 kN uniaxial press. The system was first evacuated and a uniaxial pressure of 80 MPa was applied. A pulsed current was then activated and maintained until the densification rate was negligible, as indicated by the real-time output of the shrinkage recode system. The shrinkage was monitored by a linear gauge which measured the vertical displacement. The temperatures were measured by a pyrometer focused on the surface of the graphite die. At the end of the process, the pulsed current was turned off and the sample was cooled to room temperature. The process was carried out under vacuum at a pressure of 4×10^{-2} Torr.

The relative density of the sintered sample was measured by the Archimedes method. The samples for the microstructural examination were polished and etched using a solution of HF (10 vol%), HNO_3 (40 vol%) and H_2O (50 vol%) for 1–2 min at room temperature. Compositional and microstructural analyses of the powders and the products were conducted by X-ray diffraction (XRD), scanning electron microscopy (SEM) with energy dispersive spectroscopy (EDS), and field emission scanning electron microscopy (FE-SEM). The Vickers hardness was measured by performing indentations at a load of 20 kg_f and a dwell time of 15 s.

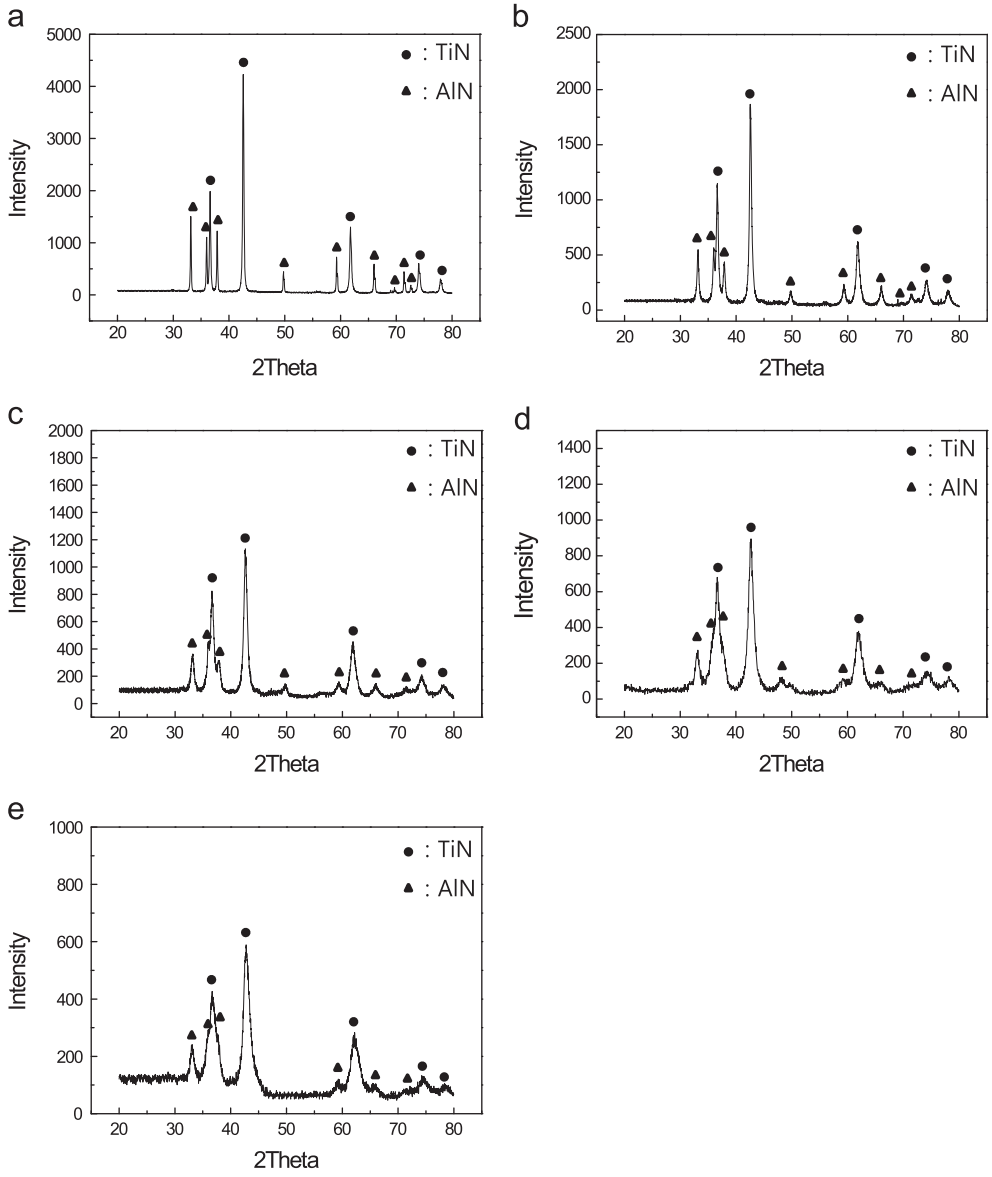

Fig. 3. X-ray diffraction patterns of the TiN–AlN powder after high-energy milling for various durations: (a) as-received, (b) milled for 1 h, (c) milled for 4 h, (d) milled for 10 h, and (e) milled for 40 h.

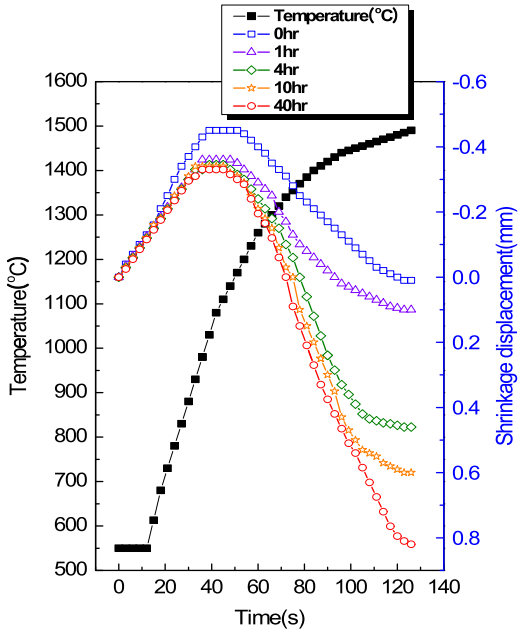

Fig. 4. Shrinkage displacement–temperature curves obtained during the pulsed current activated sintering of TiN–AlN powders milled for various durations.

3. Results and discussion

Fig. 2 shows SEM images of the TiN–AlN mixture powders obtained after high-energy milling for various durations. The high-energy milling greatly refined the microstructure of the TiN and AlN particles. Nevertheless, any chemical reaction between TiN and AlN powders during the milling process was observed. Fig. 3(a–e) shows the X-ray diffraction patterns of the TiN and AlN powders after milling for 1–40 h. As marked in the patterns, they show only TiN and AlN peaks, suggesting the absence of a chemical reaction between them. However, both the TiN and AlN peaks are broadened due to strain and crystallite refinement and their broadening increases with increasing milling time. The milling process is known to introduce impurities from the ball and/or container. However, in this study, peaks other than TiN and AlN were not identified. Therefore, it can be concluded that no major contamination occurred.

The TiN crystallite sizes calculated using Suryanarayana and Grant Norton′s formula were 56, 21, 15 and 10 nm after milling for 1, 4, 10, and 40 h, respectively. The AlN crystallite sizes were 26, 22, 21, and 16 nm after milling for 1, 4, 10, and 40 h, respectively. The above results suggest that the milling effectively

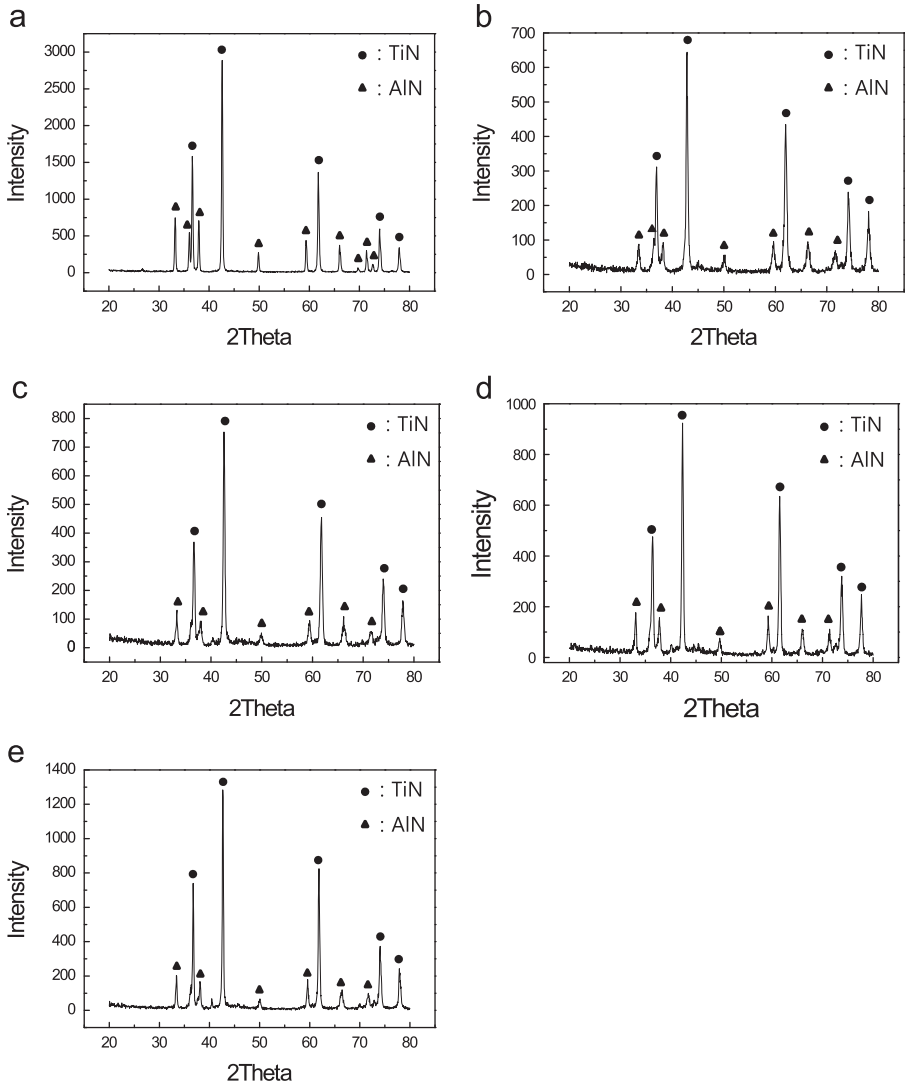

Fig. 5. X-ray diffraction patterns of the sintered compacts of TiN–AlN powders after milling for various durations: (a) as-received, (b) milled for 1 h, (c) milled for 4 h, (d) milled for10 h, and (e) milled for 40 h.

refined the microstructure of the TiN and AlN raw powders which may help the subsequent densification process thereafter.

The shrinkage displacement–time (temperature) curve provides important information concerning the consolidation behavior. Fig. 4 shows the shrinkage record of the TiN–AlN compacts obtained under an applied pressure of 80 MPa. After the initial expansion period, the compact shrinks rapidly depending on the milling conditions. The amount of shrinkage displacement, which is an indication of the degree of densification, increases with increasing milling time. It is seen that the shrinkage-onset temperature decreases with increasing milling time. In addition, the time required to obtain a certain shrinkage displacement becomes shorter as the milling time increases. Similarly, the temperature required to obtain a certain shrinkage displacement also decreases with increasing milling time. This demonstrates the effectiveness of the preparatory milling process on the densification of the TiN–AlN powders. It is considered that the milling effect increases because both the driving force for sintering and the powder contact points for the atomic diffusion route increase.

Fig. 5 shows the X-ray diffraction patterns of the sintered TiN–AlN powders. All peaks are indexed to TiN and AlN. The broader peaks observed after milling were reduced significantly suggesting that grain growth occurs during sintering. Fig. 6(a–e) shows SEM images of the polished surface of the sintered TiN–AlN composites. The reduction of the pore volume and grain size with increasing milling time is obvious. The sintered compacts possess a nano-scale grain size even though they are obviously larger than the milled powders. In this regard, it is interesting to refer to our previous study of TiN using PCAS. Unlike the results of this study, the average crystallite size of the sintered TiN was several micrometers, which was significantly larger than that of the starting powders. [13]. In view of this, it is believed that a nanostructured TiN–AlN composite was obtained since finely dispersed AlN and TiN powders acted to inhibit the grain growth of each other during the sintering. The relative densities of TiN–AlN sintered at 1490 °C from the powders milled for 0, 1, 4, 10 and 40 h are 80%, 92%, 96%, 99% and 99%, respectively.

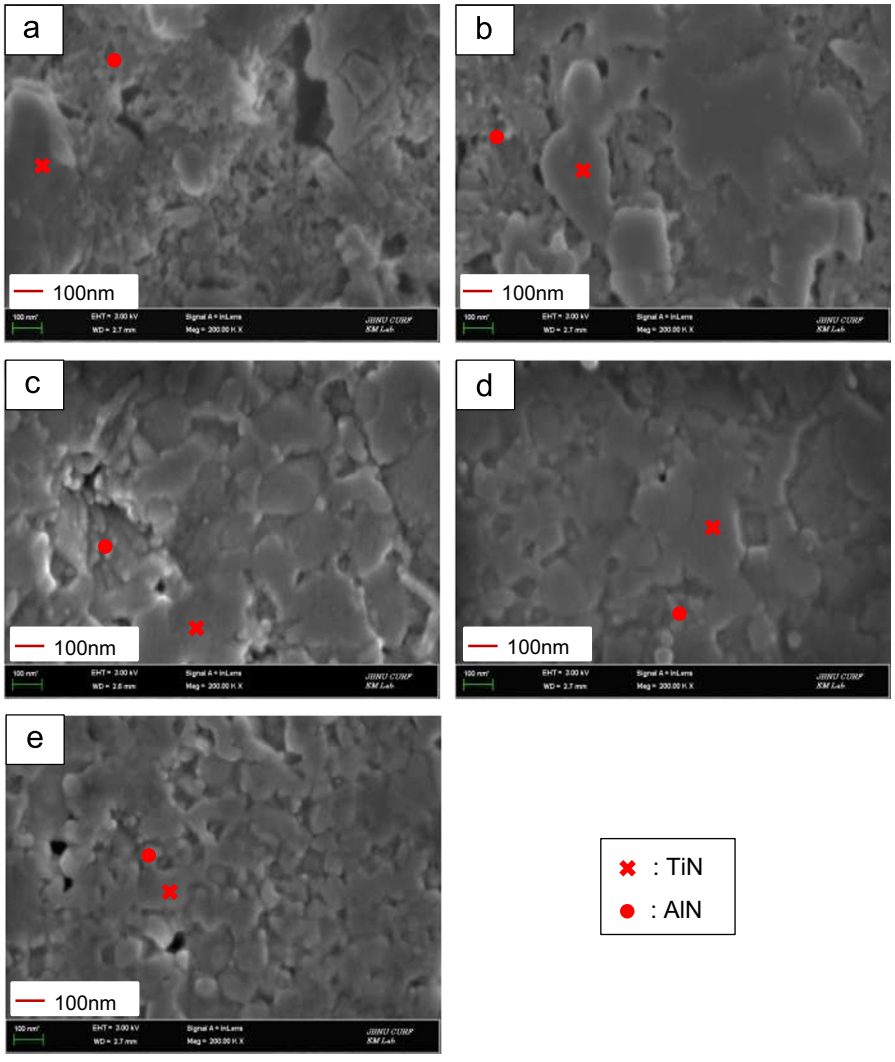

Fig. 6. SEM micrographs showing the polished and etched surface of TiN–AlN compacts: (a) as-received (b) milled for 1 h, (c) milled for 4 h, (d) milled for 10 h, and (e) milled for 40 h.

The highly dense TiN–AlN composite was sintered within 3 min by pulsed current activated heating. The role of the pulse current in sintering has been the subject of several studies conducted to explain the observed enhancement of sintering and the improved characteristics of the products. The role played by the current has been variously interpreted with the effect being explained in terms of the fast heating rate due to Joule heating, the presence of plasma in the pores separating powder particles [20], and the intrinsic contribution of the current to mass transport [21–23].

The Vickers hardness and fracture toughness were measured to evaluate the mechanical properties of the TiN–AlN composites. The Vickers hardness measurements were performed on polished sections of the TiN–AlN composites using a 20 kg_f load and a 15 s dwell time. Indentations with large enough loads produced median cracks around the indent. From the length of these cracks, the fracture toughness values can be determined using the following formula proposed by Niihara et al. [24]

$$K_{IC} = 0.203(c/a)^{-3/2} H_V a^{1/2} \quad (2)$$

Here, c is the trace length of the crack measured from the center of the indentation, a is one half of the average length for the two indent diagonals, and H_v is the hardness.

The hardness of the sintered TiN–AlN composite increased as the milling time increased without a loss of the fracture toughness. This effect may be attributed to enhanced densification. The hardness and fracture toughness values of TiN–AlN sintered at 1490 °C using powders milled for 0, 1, 4, 10, and 40 h are 470, 1044, 1474, 1831, and 1839 kg/mm^2 and 2.9 3.1, 3.2, 3.3, and 3.3 Mpa m$^{1/2}$, respectively. The hardness of the TiN–AlN composite sintered from powders milled for 40 h is significantly higher than that of TiN previously reported (1486 kg/mm^2) [13] possibly due to grain size refinement. It was believed that the grain size refinement of TiN–AlN composite was possible because the coexistence of TiN or AlN grains is expected to act as an obstruction to the individual grain growth of each nitride phases. The Vickers hardness indentations on the TiN–AlN samples sintered from the powders milled for 0, 1, 4, and 10 h are shown in Fig. 7(a–e), which typically show one to three additional cracks propagating radially from the indentation.

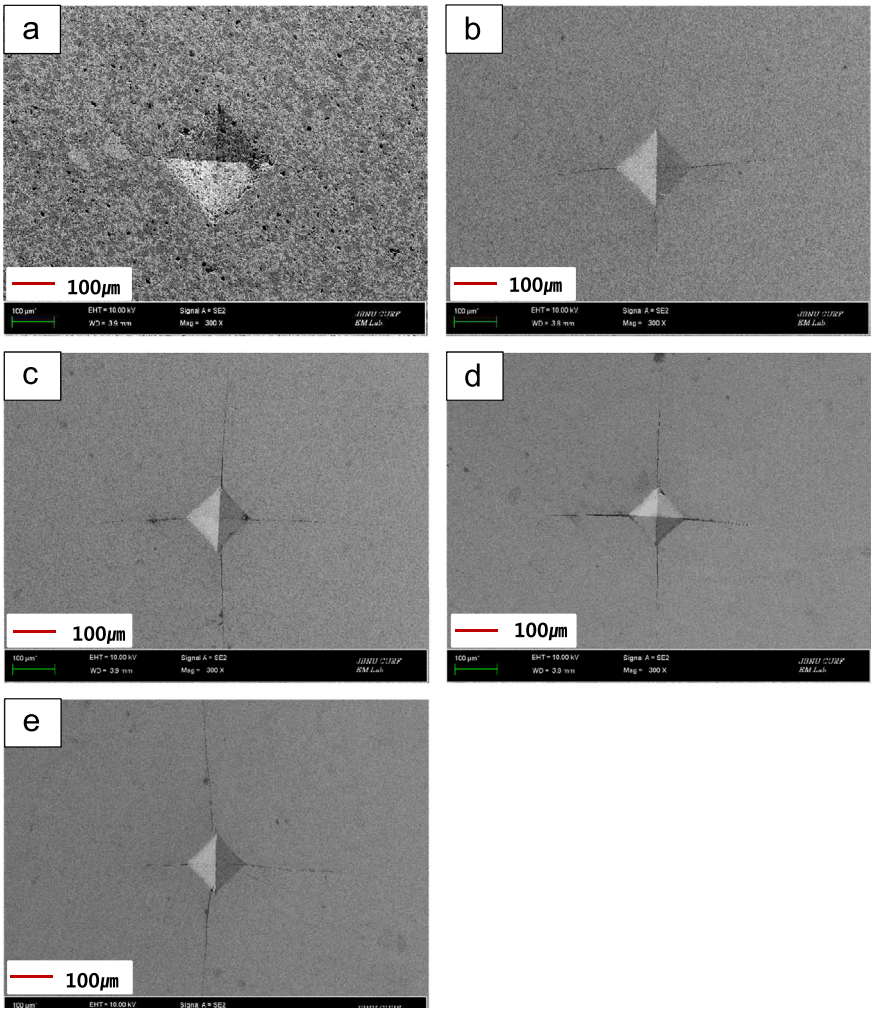

Fig. 7. Vickers hardness indentations of the TiN–AlN composites sintered using TiN–AlN powders after milling for various durations: (a) as-received, (b) milled for 1 h, (c) milled for 4 h, (d) milled for 10 h, and (e) milled for 40 h.

4. Conclusions

A mixture of commercial TiN and AlN powders was high-energy ball milled for various durations and consolidated without a binder using the pulsed current activated sintering method (PCAS). The ball milling substantially refined the crystallite structure of the TiN and AlN powders and greatly facilitated the subsequent densification process. The shrinkage-onset temperature of the TiN–AlN powders was reduced by milling for 40 h from 1200 °C to 1100 °C. A nanostructured TiN–AlN composite can be obtained by the addition of AlN to TiN. The fracture toughness and Vickers hardness values of the TiN–AlN compacts sintered at 1490 °C were 2.9, 3.1, 3.2, 3.3, and 3.3 Mpa $m^{1/2}$ and 470, 1044, 1474, 1831, and 1839 kg mm^{-2} using powders milled for 0, 1, 4, 10, and 40 h, respectively. Their corresponding relative densities were approximately 80%, 92%, 96%, 99%, and 99%. The micro-hardness values of the sintered TiN–AlN composites were higher than that of monolithic TiN due to the refinement of grain size.

Acknowledgments

This study was supported by a Grant from the basic research project of the Korea Institute of Geoscience and Mineral Resources and Following are results of a study on the "Leaders Industry-university Cooperation" Project, supported by the Ministry of Education, Science & Technology (MEST).

References

[1] K. Vandierendonck, M. Van Stapen, Study of the performance of PVD and PCVD coated cermets for different cutting applications, Surface and Coatings Technology 97 (1–3) (1997) 218–223.
[2] V. Hlavacek, J. Puszynski, Combustion synthesis of transition metal nitrides, Combustion, Explosion, and Shock Waves 10 (1996) 223–251.
[3] A.G. Merzhanov, G.G. Karyuk, I.P. Borovinskaya, V.A. Prokudina, E.G. Dyad, Titanium carbide produced by self-propagating high-temperature synthesis-valuable abrasive material, Soviet Powder Metallurgy and Metal Ceramics 20 (1981) 709–715.
[4] M. Eslamloo-Grami, Z.A. Munir, Effect of nitrogen pressure and dilute content on the combustion synthesis of titanium nitride, Journal of the American Ceramic Society 73 (8) (1990) 2222–2227.
[5] M. Eslamloo-Grami, Z.A. Munir, Effect of prosity on the combustion synthesis of titanium nitride, Journal of the American Ceramic Society 73 (5) (1990) 1235–1239.
[6] M. Shibuya, J.F. Despres, O. Odawara, Characteristic sample temperature and press during process of titanium nitride combustion synthesis with liquid nitrogen, Journal of Materials Science 33 (1998) 2573–2576.
[7] C.L. Yen, H.C. Chuang, Combustion characteristics of SHS process of titanium nitride with TiN dilution, Ceramics International 30 (5) (2004) 705–714.
[8] R.A. Andrievski, Physical–mechanical properties of nanostructured titanium nitride, Nanostructured Materials 9 (1997) 607–610.
[9] O.B. Zgalat-Lozinskii, A.V. Ragulya, V.V. Skorokhod, T.V.M. Tomila, L.I. Klochkov, V.V. Garbuz, Powder Metallurgy and Metal Ceramics 40 (9–10) (2001) 471–477.
[10] I.J. Shon, I.Y. Ko, H.S. Kang, K.T. Hong, J.M. Doh, J.K. Yoon, Rapid synthesis and consolidation of nanostructured Al_2O_3–$MgSiO_3$ composites by high frequency induction heated sintering, Metals and Materials International 18 (2012) 109–113.
[11] I.J. Shon, K.I. Na, J.M. Doh, H.K. Park, J.K. Yoon, Simultaneous synthesis and consolidation of nanocrystalline Fe_2Al_5 and Fe_2Al_5–Al_2O_3 by pulsed current activated sintering and their mechanical properties, Metals and Materials International 19 (2013) 99–103.
[12] I.J. Shon, K.I. Na, I.Y. Ko, J.M. Doh, J.K. Yoon, Effect of $FeAl_3$ on properties of (W,Ti)C–$FeAl_3$ hard materials consolidated by a pulsed current activated sintering methode, Ceramics International 38 (2012) 5133–5138.
[13] Wonbaek Kim, Jae-Won Lim, Hyun-Su Oh, In-Jin Shon, The effect of ball milling on the mechanical properties of TiN consolidation by pulsed current activated sintering, Journal of Alloys and Compounds 574 (2013) 260–265.
[14] M. Sherif El-Eskandarany, Structure and properties of nanocrystalline TiC full-density bulk alloy consolidated from mechanically reacted powders, Journal of Alloys and Compounds 305 (2000) 225–238.
[15] L. Fu, L.H. Cao, Y.S. Fan, Two-step synthesis of nanostructured tungsten carbide–cobalt powders, Scripta Materialia 44 (2001) 1061–1068.
[16] K. Niihara, A. Nikahira, Advanced Structural Inorganic Composite, Elsevier Scientific Publishing Co., Trieste, Italy, 1990.
[17] S. Berger, R. Porat, R. Rosen, Nanocrystalline materials: a study of WC-based hard metals, Progress in Materials 42 (1997) 311–320.
[18] C.Y. Hsieh, C.N. Lin, S.L. Chung, J. Cheng, D.K. Agrawal, Microwave sintering of AlN powder synthesized by a SHS method, Journal of the European Ceramic society 27 (2007) 343–350.
[19] C. Suryanarayana, M. Grant Norton, X-ray Diffraction—A Practical Approach, Plenum Press, New York, 1998.
[20] Z. Shen, M. Johnsson, Z. Zhao, M. Nygren, Spark plasma sintering of alumina, Journal of the American Ceramic Society 85 (2002) 1921–1926.
[21] J.E. Garay, U. Anselmi-Tamburini, Z.A. Munir, S.C. Glade, P. Asoka-Kumar, Electric current enhanced defect mobility in Ni_3Ti intermetallic electric current enhanced defect mobility in Ni_3Ti intermetallics, Applied Physics Letters 85 (2004) 573–580.
[22] J.R. Friedman, J.E. Garay., U. Anselmi-Tamburini, Z.A. Munir, Modified interfacial reactions in Ag–Zn multilayers under the influence of high DC currents, Intermetallics 12 (2004) 589–596.
[23] J.E. Garay, J.E. Garay., U. Anselmi-Tamburini, Z.A. Munir, Enhanced growth of intermetallic phases in the Ni–Ti system by current effects, Acta Materialia 51 (2003) 4487–4493.
[24] K. Niihara, R. Morena, D.P.H. Hasselman, Evaluation of KIC of brittle solids by the indentation method with low crack-to-indent ratios, Journal of Materials Science Letters 1 (1982) 12–17.